Conductive Carbon Nanotubes for Semiconductor Metrology

Victor Vartanian
International SEMATECH Manufacturing Initiative, 257 Fuller Road, Ste. 2200, Albany, NY 12203

Paul McClure and Vladimir Mancevski
Xidex Corporation, 8906 Wall Street, Suite 703, Austin, Texas 78754

Joseph J. Kopanski
NIST, Electronics Materials Characterization, Semiconductor Electronics Division, 100 Bureau Drive Stop 8120, Gaithersburg, MD 20899-8120

Philip D. Rack
Materials Science and Engineering, the University of Tennessee, 603 Dougherty Hall, Knoxville TN, 37996-2200

Ilona Sitnitsky, Matthew D. Bresin, Vince LaBella, and Kathleen Dunn
College of Nanoscale Science and Engineering, University at Albany – SUNY, Albany, NY 12203

Abstract

This paper presents an evaluation of e-beam assisted deposition and welding of conductive carbon nanotube (c-CNT) tips for electrical scanning probe microscope measurements. Variations in CNT tip conductivity and contact resistance during fabrication were determined as a function of tip geometry using tunneling AFM (TUNA). Conductive CNT tips were used to measure 2D dopant concentration as a function of annealing conditions in BF_2-implanted samples.

Keywords: Carbon nanotubes, ultra-shallow junction, semiconductor, laser anneal, scanning probe microscopy, scanning capacitance microscopy, scanning Kelvin force microscopy, dopant activation, low-k dielectric, FinFET

Introduction

Shrinking device features demand dopant metrology with sub-10 nm spatial resolution combined with low detection limits (<1e15 atoms/cm^3). The 2009 *International Technology Roadmap for Semiconductors* (ITRS) requirements for lateral/depth spatial resolution for 2D/3D dopant profiles in 2012 is 2.4 nm [2009 Metrology Update, ITRS, Table 1].

Year of Production	2009	2010	2011	2012	2013	2014	2015
Dopant atom	P, As, B	P, As, B	P, As, B	P, As, B	P, As, B	P, As, B	P, As, B
Drain extension X_j (nm) for bulk MPU/ASIC [A]	13	12	10.5	9.5	8.7	8	7.3
Extension lateral abruptness for bulk MPU/ASIC (nm/decade) [C]	3.5	3.2	2.8	2.4	2.3	2	1.8
Lateral/depth spatial resolution for 2D/3D dopant profile (nm)	3.5	3.2	2.8	2.4	2.3	2	1.8
At-line dopant concentration precision (across concentration range) [D]	4%	2%	2%	2%	2%	2%	2%

Table 1: 2009 Metrology Update, ITRS.

The scaling of CMOS transistors below a 100 nm channel length has led to shallower junctions and higher channel doping concentrations for better short channel control. With increasingly smaller dimensions, dopant metrology requires better measurement accuracy and lower uncertainty. Conventional techniques such as secondary ion mass spectrometry (SIMS) have been widely used to evaluate dopant profiles and depths, but this is a destructive and time-intensive technique and does not distinguish electrically active, substitutional dopants from non-electrically active interstitial dopants.
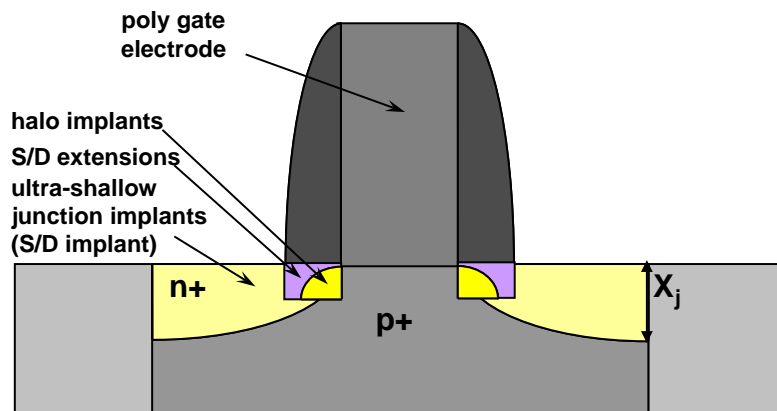
Figure 1: CMOS USJ dopants for improved short channel device performance.

While SIMS and electron microscopy have been developed for two-dimensional profiling, scanning probe microscopy (SPM) techniques have become extremely attractive because of very high spatial resolution and the ability to obtain detailed maps of topography, electrical properties, magnetic and electrostatic forces, and other properties of 2D devices. SPM-based 2D dopant profiling methods include tunneling

atomic force microscopy (TUNA), scanning capacitance microscopy (SCM), scanning spreading resistance microscopy (SSRM), and scanning surface potential microscopy (SSPM), otherwise known as Kelvin force microscopy (KFM). The table below summarizes these techniques.

| SPM Technique	Mode	Probe	Measured Quantity
TUNA or C-AFM	Contact-AFM	Metal-coated Si or Metallic; CNT	# of doping atoms
			I-V spectra
SCM	Contact-AFM	Metal-coated Si or Metallic; CNT	Depletion Capacitance
			C-V spectra
SSRM	Contact-AFM	Diamond coated Si; CNT	Electrical Resistance
			I-V spectra
SSPM or KFM	Intermittent Contact-AFM	Metal-coated Si or Metallic; CNT	Electrostatic potential
			Work function

Table 2: Summary of SPM techniques.

The primary objective of this work is to produce conductive CNT SPM tips supported on Si cantilevers suitable for nanometer-scale measurements of carrier concentration profiles. SPM-based 2D dopant profiling methods to be studied include TUNA and SCM. Xidex, the University of Tennessee at Knoxville, the College of Nanoscale Science and Engineering, and the National Institute of Standards and Technology (NIST) prepared and physically characterized conductive CNT SPM tips using focused ion beam (FIB), scanning electron microscopy (SEM), transmission electron microscopy (TEM), scanning tunneling microscopy (STM), and atomic force microscopy (AFM). NIST developed and electrically characterized CNT tips primarily using current voltage (IV) measurements (TUNA). CNT tip conductivity variation was also determined to assess statistical variations. Variations in contact resistance between the CNT and AFM cantilevers were also determined, as well as CNT-to-CNT conductivity.

In an earlier phase of work, Xidex initially investigated manual mounting and direct growth of CNT tips, and manufacturing techniques were to be improved using electron beam-induced deposition (EBID). However, manual mounting of the CNT tips was a better short-term solution that allowed different cantilever substrates to be investigated, such as Si-based cantilevers coated with different metals. Direct growth of CNT tips is more scaleable but requires more process development to grow CNTs on a metal-coated Si base. The CNT tips in this work had diameters of 7 to 20 nm and lengths of 56 to 750 nm.

Manually Mounted CNT Tips - Conductive CNT tips provided to NIST at the start of the project were fabricated by manually mounting a CNT on the apex of a Si AFM tip, as shown in Figure 1. The manually mounted CNTs are initially held in place by van der Waals attraction and then welded to the AFM tip using carbon

EBID. The attachment strength, and hence longevity of the manually mounted CNT tips, can approach that of grown CNTs. However manual mounting is a less scaleable process. Multi-walled CNT tips of this kind are shown in Figure 2 (a four-walled CNT is shown on the right). The physical characteristics of the conductive CNT tips were investigated using TEM and SEM. TEM images of Xidex's CNT tips typically showed a diameter of <10 nm, with four cylindrical shells. The CNTs shown in Figure 2 have carbon deposited on the outer walls resulting from the TEM preparation methods. The TEM images also showed that the CNTs were crystalline and without defects, implying that these CNTs would have good electrical properties.
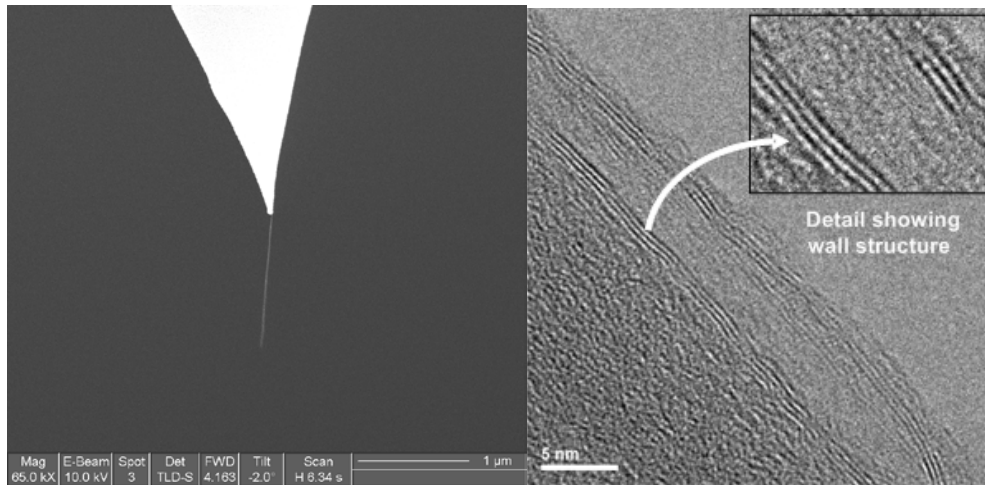

Figure 2: Manually mounted SPM tips (left). TEM of four-walled CNT (right).

E-Beam Assisted Metal Deposition

An alternative way of fabricating CNT tips is to first grow the CNT and then improve the electrical connectivity between the CNT and the substrate by coating the entire CNT and the substrate with a layer of metal. This approach is potentially more scaleable (large-scale manufacturability) than the method of electron beam welding.

Fabrication begins by first coating a Si tip with an Ag layer to make the Si more conductive, followed by coating the tip with a proprietary catalyst mix. Then the CNT tip is grown directly from the tip, as shown in Figure 3.
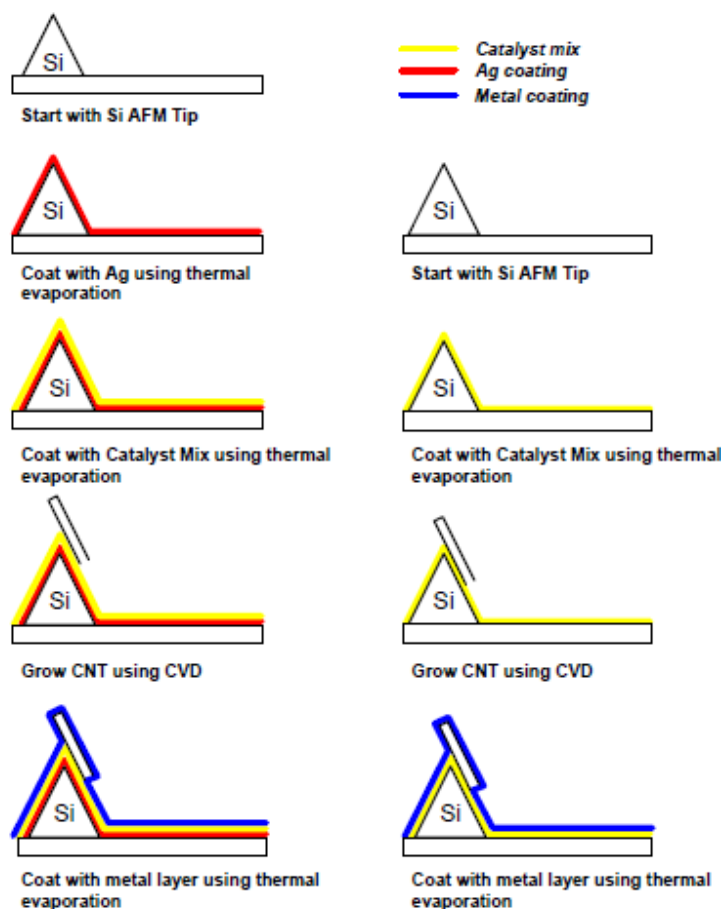
Figure 3: Various metal coating strategies to improve conductivity.

The mechanism of EBID is depicted in Figure 4, in which e-beam assisted metal deposition is used to weld the CNT to the substrate. A gaseous precursor flows through a gas injection system (GIS) and subsequently adsorbs on the substrate (A). Electrons break precursor bonds near the beam (~10 nm deposit resolution), resulting in decomposition (B). Target and impurity atoms are incorporated into the film, while volatile byproducts desorb and are removed by the pumping system (C). If the precursor gas is an etchant, the decomposition products form reactive radicals that volatilize the surface, etching the material.
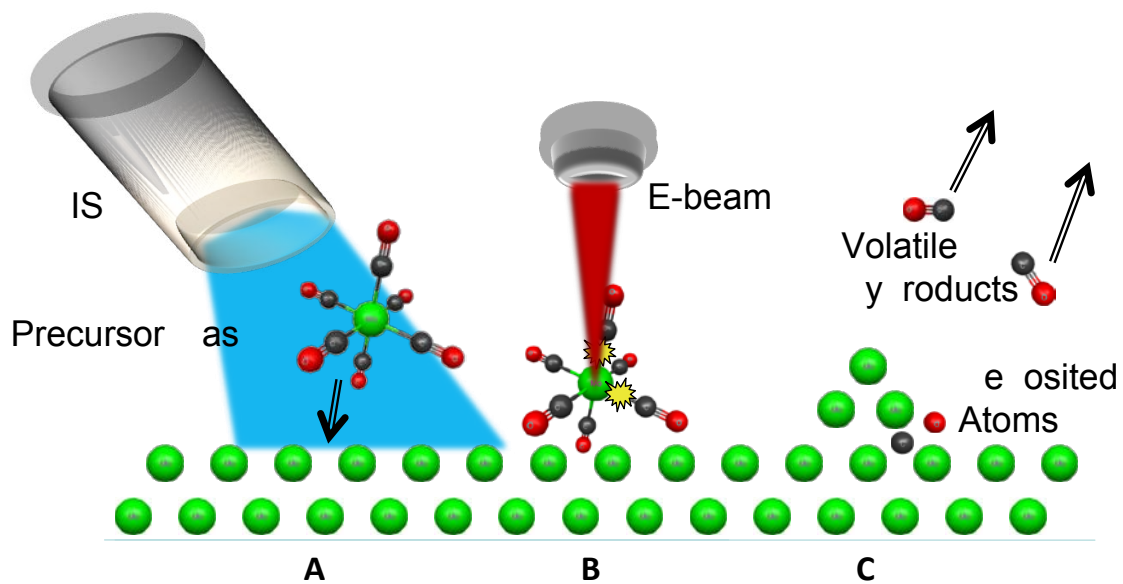
Figure 4: E-beam-assisted welding.

E-beam assisted dielectric deposition onto the CNT tip (excluding the tip apex) was investigated to reduce the parasitic capacitance of the tip with respect to the sample. Platinum or gold (Figure 5) was deposited between the tip and the cantilever to reduce the contact resistance; good local contact was made, with no perceptible deposition on the CNT. Ion milling was also investigated as a means to support manufacturing of well aligned CNT tips as well as the use of e-beam assisted etching to remove carbon contamination from the CNT. Approaches to replace the expensive ion mill drilling with e-beam assisted etching of metal, silicon, or metal-coated silicon were also studied.
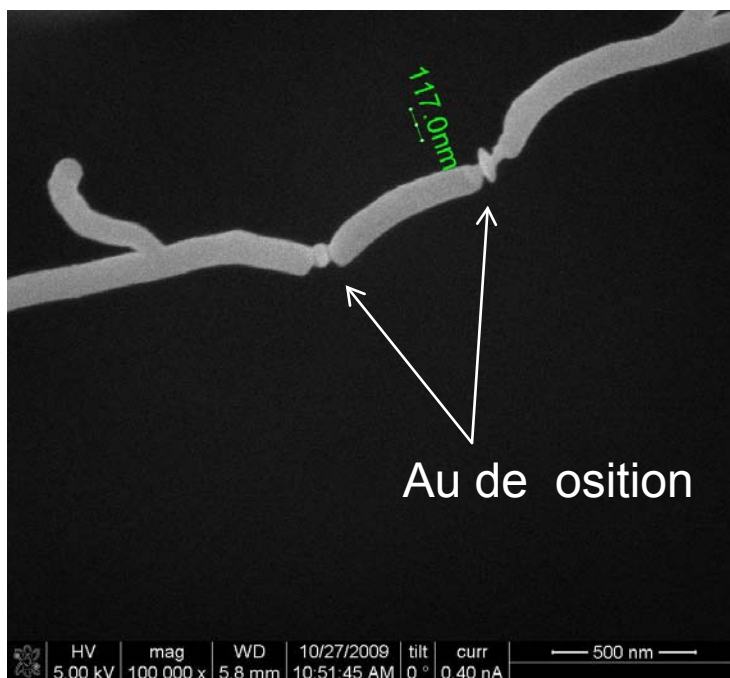
Figure 5: Au (117 nm diameter) deposited on CNT using an organic precursor containing gold.

Demonstration of Electrically Shielded CNT Tips

The feasibility of making electrically shielded CNT tips as proposed above was also demonstrated [1]. First, a CNT was grown on a Si tip followed by the deposition of a SiO layer, uniformly coating the CNT and the Si tip. The SiO was deposited using thermal evaporation. Next, using the FIB tool, only the apex of the CNT tip was etched, making the apex electrically conductive while the rest of the CNT and the Si tip were shielded with the dielectric layer. Bundles of CNTs were used instead of individual CNTs on a Si tip, as shown in Figure 6, illustrating that the SiO can be selectively etched without damaging the CNT. Figure 6 shows the results of etching to expose the CNT tip coated with SiO.
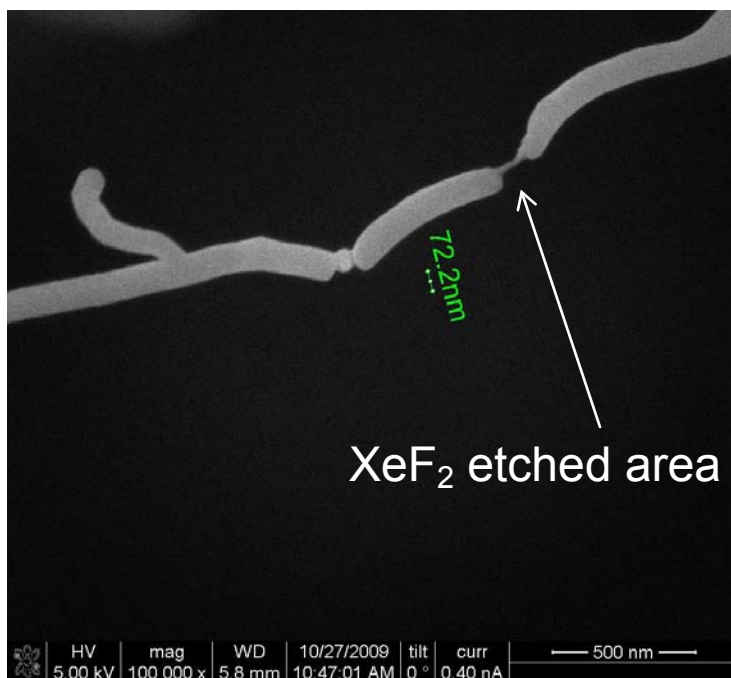
Figure 6: Selective oxide etch on CNT using XeF_2.

EBID, performed is depicted in Figure 7, involved applying a localized, thin metal contact to increase contact area and tip stability and lower tip-to-base resistance. Oxide may be grown to provide electrical shielding to reduce parasitic capacitance between the probe and sample surface. A localized and chemically selective etch method is used to release the CNT from the oxide shield.
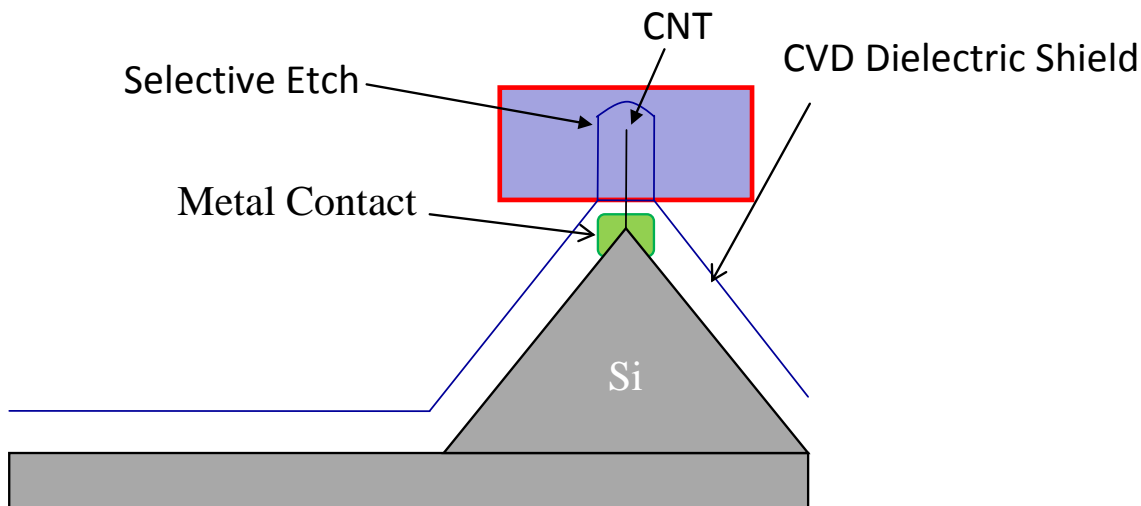

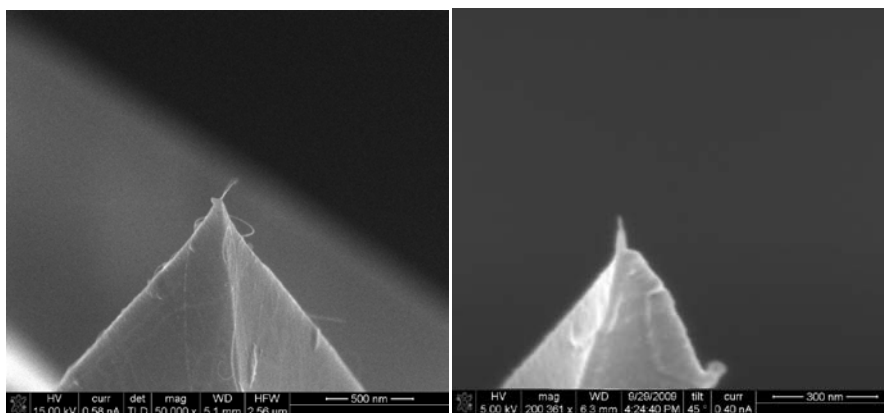Figure 7: E-beam induced deposition and etching.

Figure 8: Pt contact deposited between CNT tip and Si cantilever to reduce contact resistance (left). CVD dielectric shield deposited on CNT tip and AFM cantilever to reduce stray capacitance, followed by selective dielectric etching by XeF_2 to expose CNT (right).

Schottky barrier resistance in conventional CNT-to-tip approaches, though expected, does not preclude the use of the CNT as an electrical probe. Schottky barrier resistance necessitates that greater bias voltage be used for electrical measurements, decreasing dynamic range and sensitivity. Additional data deconvolution must be performed following the electrical measurement. Thus, reducing Schottky barrier resistance is critical to improving probe performance. TUNA (IV measurements) results showing the effect of Pt welding on electrical characteristics of a W-CNT-W circuit connection are shown in Figure 9. The resistivity of the circuit decreased after Pt welding of the W-CNT contacts, and the Schottky barrier was almost eliminated. Even for a completely Pt-coated CNT, there are still non-linearities in the IV curve.
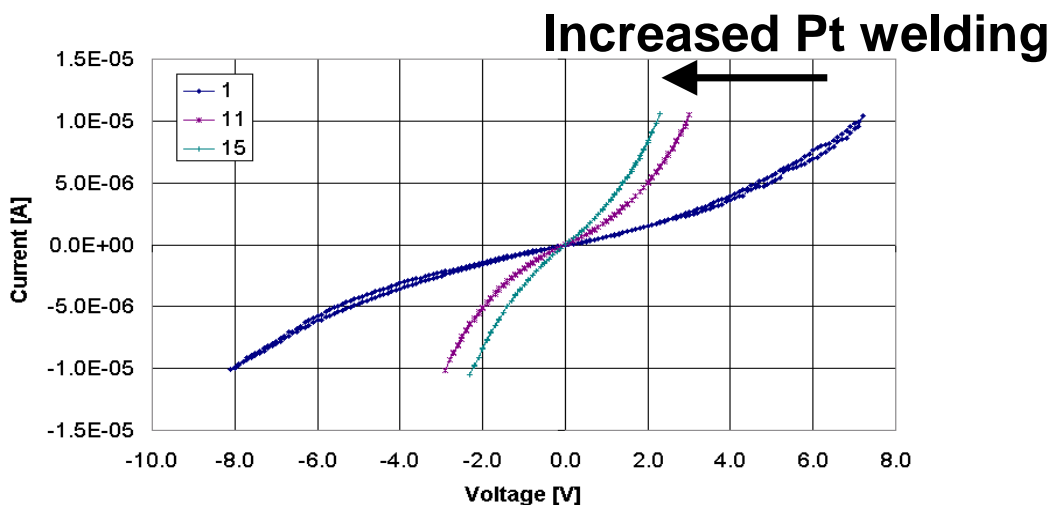

Figure 9: Typical IV curves for the assembled CNT-W connection showing that resistivity decreases after welding the CNT with increasing amounts of Pt.

With the CNT, the IV curve characteristics of a CNT-terminated tip is rectifying (highly asymmetric between positive and negative voltages) when contacting the Au film (Figure 10). The IV curve shown in Figure 10, where the CNT tip is contacting the Al film, was ohmic (symmetric), although slightly S-shaped. This implies that the rectification is at the CNT-to-film contact since this is the only parameter that changes between the two IV curves. The CNT-Au film diode has about a -0.5 V turn-on voltage and a forward resistance of 9×10^5 Ω. The CNT-Al contact has a resistance of about 3×10^5 Ω. It is unclear how much of this resistance is due to the CNT, the CNT-tip contact, and the spreading resistance in the silicon cantilever. For these initial measurements, priority was given to preserving the CNT tip; therefore, the amount of force and current that passed through the tips was critical. The measurements were repeated at a higher force and higher voltages to ensure that the resistance was not being dominated by contact effects, specifically organic contamination, oxide, or moisture at the CNT-to-film interface.
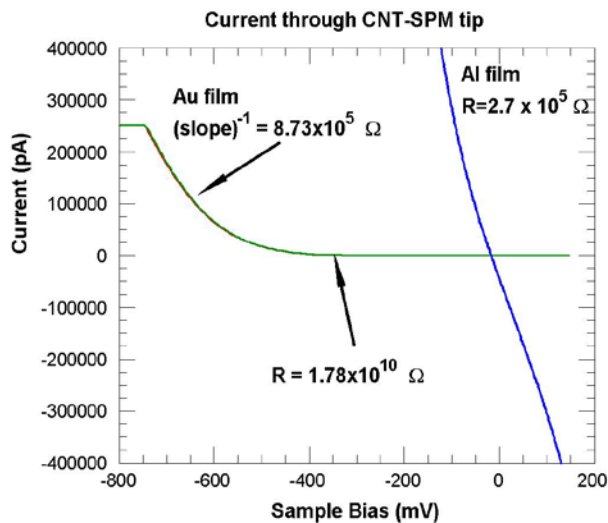

Figure 10: TUNA CNT characterization of tip resistance using showing various behavior at different applied voltages.

Evolution of IV Characteristics in TUNA Measurements of CNT-Terminated Tips
Although the CNT-terminated tips did not, in general, have linear IV characteristics, their behavior changed as progressively larger voltages were applied between the tip and sample. To preserve the tips from possible damage from excess current flow, initial measurements were made with small applied voltages ($\pm$ 100 mV). Many, but not all, tips initially exhibited a capacitive IV curve (i.e., constant current proportional to dV/dt that changed signs when the voltage sweep direction was reversed), as in Figure 11 (left). Applying a higher voltage ($\pm$ 1V) usually produced a more resistive IV curve characteristic with a high resistance, on the order of 1E+09 Ω, as in Figure 11 (center). Finally, extending the voltage range to $\pm$ 5 V or higher usually caused a contact to "form," resulting in more current flow, as in Figure 11 (right). This IV curve characteristic was usually slightly asymmetrical, with the resistance in the forward region as low as 1E+05 Ω. Its magnitude decreased over time or suddenly if the maximum

voltage range was decreased. Sufficiently high applied voltages result in a diode-like IV behavior. The effect of "forming" the contact was repeatable when the probe was withdrawn and then re-engaged to the contact.

The diode-like behavior is not expected for a CNT-to-Au contact. The work function of Au is 5.1 eV; the work function of CNTs has been reported between 4.95 and 5.10 eV [2]. However, because the diode is not strongly asymmetrical, the rectification (greater current flow for one voltage polarity versus the opposite polarity) may be due to organic contamination at the CNT-Au junction, which limits current flow at low voltages. The IV curves of at least one of the CNT-to-Al contacts exhibited more S-shaped behavior than diode behavior. This implies that rectification is at the CNT-to-film contact, since this was the only difference between the two IV curves.

The evolution of IV characteristics is not unusual. It is commonly observed with TUNA using small area contacts and surfaces exposed to atmosphere. The high electric fields at the tip terminus can result in local rapid oxidation or the rapid deposition of organic films. These tend to increase the measured resistance. The formation of a better contact at higher applied voltages is the result of the higher current temporarily overcoming this layer of organic contamination/oxide/moisture.
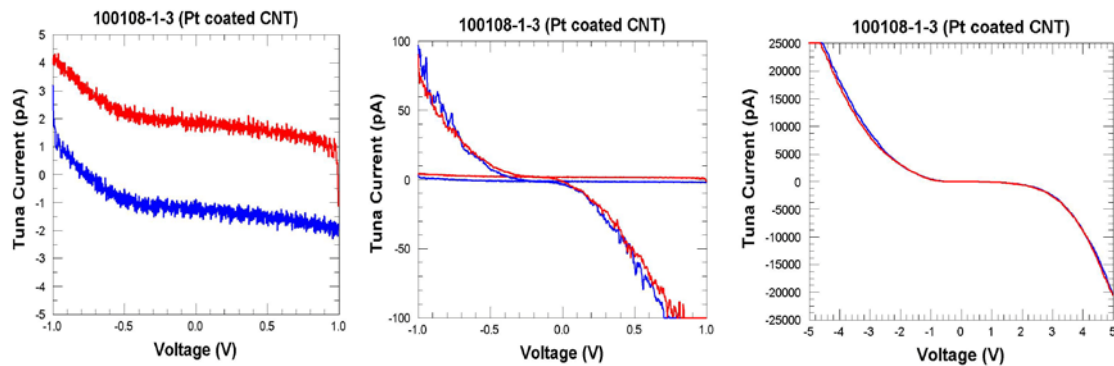

Figure 11: TUNA CNT characterization of tip resistance showing various behavior at different applied voltages.

Figure 12 (left) shows stable diode-like characteristics at higher applied voltages. The turn-on voltage decreases with time at stress, and forward resistance is relatively low at 100–500 kΩ. Figure 12 (right) shows the IV of CNT tips at low applied voltages. This is in the reverse bias region of the diodes with low current flows.
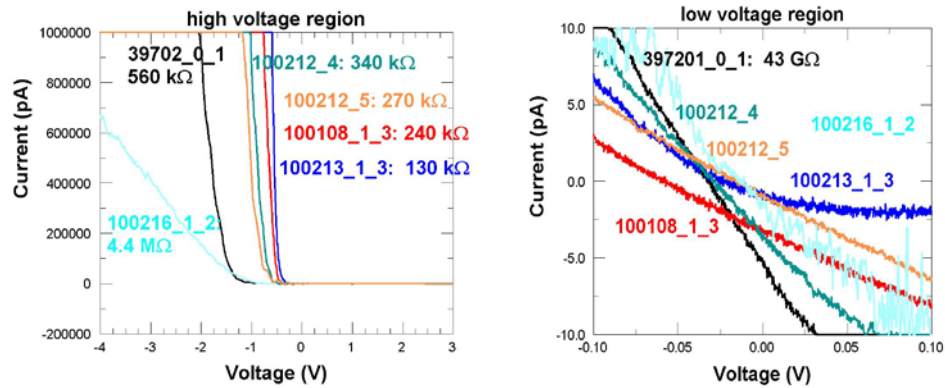
Figure 12: Stable diode-like characteristics at higher applied voltages (left) and TUNA IV curves of CNT tips at low applied voltages (right) in the reverse bias region.

SCM Sample Preparation

As SCM is a surface-sensitive technique, sample preparation is important to ensure the quality of SCM measurements. The sample surface can be damaged by polishing, producing surface roughness and surface charges that can affect the capacitance sensor and resulting in tip physical properties are not ideal. Sample preparation is also a critical part in achieving high resolution measurements in SCM. It took several years since the first application of SCM to obtain a cross-sectional 2D SCM image of the P+P implant [3]. Originally, the polishing techniques applied in SEM were used for SCM samples [4] [5]. The sample preparation technique must satisfy several requirements including having good oxide quality, an artifact-free surfaces, and good surface morphology repeatability, as well as being cost effective [6]. Furthermore, the sample polishing finishing procedure using colloidal silica is critical because it produces a thin insulating layer on the sample, the result of an oxidative reaction between hydroxide and silicon [4] [5] [7]. The final stage in sample preparation is the oxidation of the surface using ultraviolet (UV)-generated ozone, as capacitance measurements are impossible without an oxide layer above and a metal layer, such as aluminum, below. The cross-section of the sample after preparation is illustrated in Figure 13.
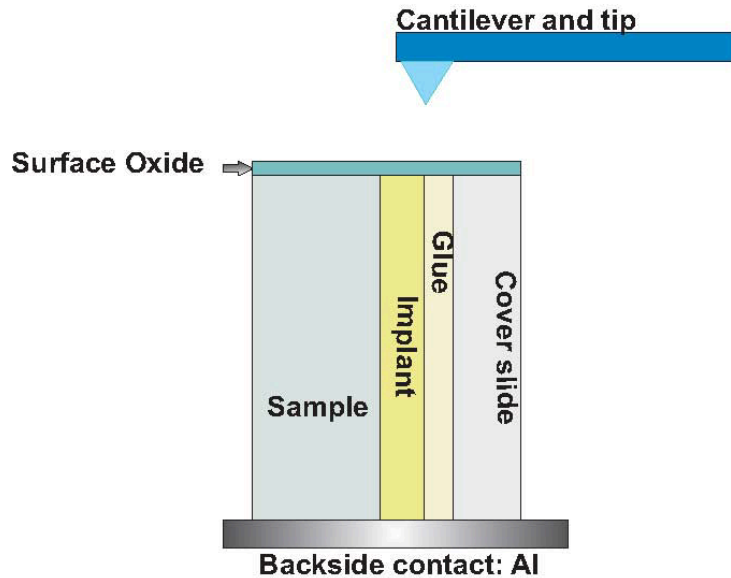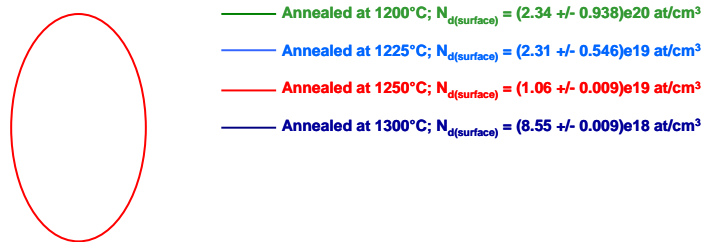
Figure 13: SCM for sample preparation showing oxide deposition on top surface of the sample (rotated to allow scanning through the sample cross-section) and backside Al deposition for ohmic contact.

Data and Analysis of BF$_2$ Laser-Annealed Implant Samples

A laser-annealed implant wafer (BF$_2$, at 2.0e15 at/cm^2) was analyzed using a solid Pt wire tip Figure 13 (top). The wafer was laser-annealed at temperatures of 1200°C, 1225°C, 1250°C, and 1300°C on four sections of the wafer. SCM analysis showed that the section of the wafer that was annealed at 1200°C had a higher surface doping concentration than the section annealed at 1300°C [7] [8]. This observation suggests that dopants diffused less at lower laser annealing temperatures. Figure 14 (bottom) presents data obtained on an unannealed wafer, showing a higher surface concentration.

Annealed at 1200°C; $N_{d(surface)}$ = (2.34 +/- 0.938)e20 at/cm^3

Annealed at 1225°C; $N_{d(surface)}$ = (2.31 +/- 0.546)e19 at/cm^3

Annealed at 1250°C; $N_{d(surface)}$ = (1.06 +/- 0.009)e19 at/cm^3

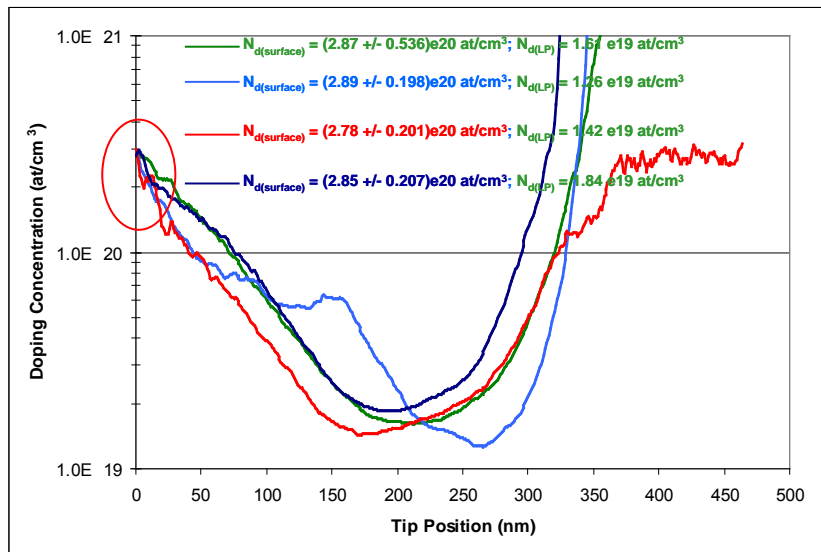Annealed at 1300°C; $N_{d(surface)}$ = (8.55 +/- 0.009)e18 at/cm^3

Figure 14: SCM scans comparing dopant diffusion at surface for the laser-annealed samples (top) and unannealed samples (bottom).

Similar measurements were made by SCM to measure doped FinFET structures (Figure 15). AFM and SCM images of B-doped and annealed scatterometry array structures are shown in Figure 16. The FinFET structure is cross-sectioned and rotated 90°, such that the fins are perpendicular to the scan direction. The bright contrast image shows height in the AFM and capacitance in the SCM, indicating a higher dose. Using CNTs, the limited spatial resolution and sensitivity would be improved; this is planned for the near future.
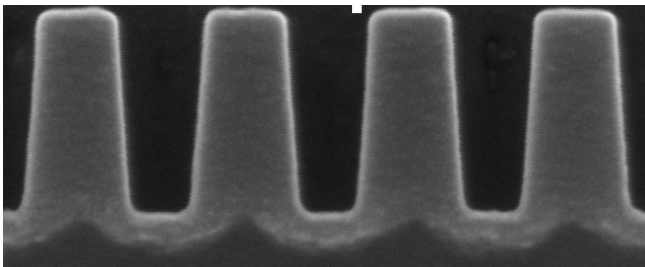

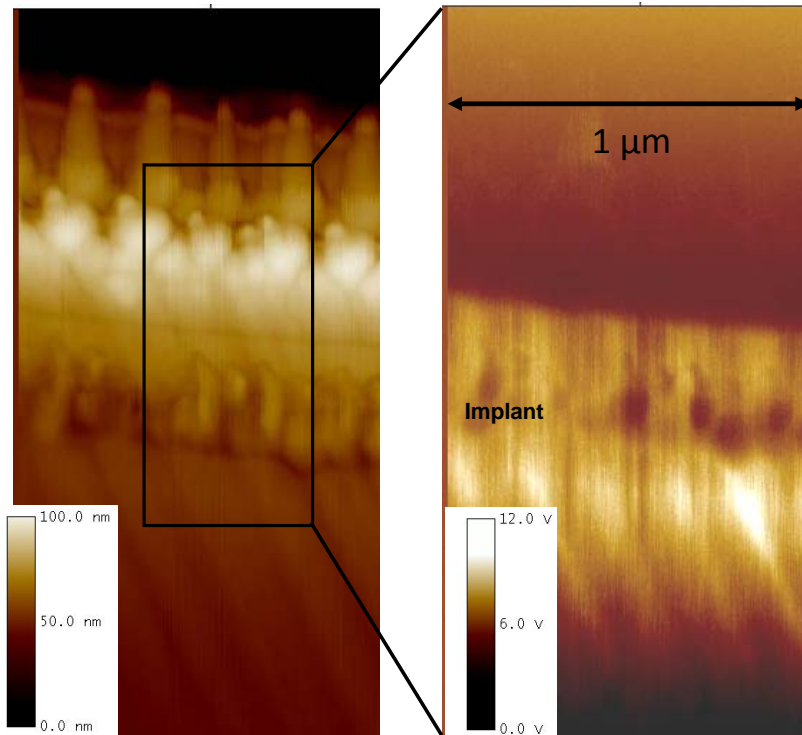Figure 15: TEM of 40 nm tall doped FinFET.

Figure 16: AFM (left) and SCM (right) images of implanted FinFET scatterometry array structures.

REFERENCES

.

[1] SBIR Phase I: Conductive Shielded Carbon Nanotube Probes. National Science Foundation Grant # 0945206, Jan. 1 – June 30, 2010.

[2] M. Shiraishi and M. Ata, "Work function of carbon nanotubes," Carbon 39, 1913-1917 (2001).

[3] A. Erickson, L. Sadwick, G. Neubauer, J. Kopanski, D. Adderton, and M. Rogers "Quantitative scanning capacitance microscopy analysis of two-dimensional dopant concentrations at nanoscale dimensions," J. Electron. Mater., 25, p. 301, (1996).

[4] J. J. Kopanski, J. F. Marchiando, D. W. Berning, R. Alvis, and H. E. Smith, "Scanning capacitance microscopy measurement of two-dimensional dopant profiles across junctions," J. Vac. Sci. Technol. B, 16, p. 339, (1998).

[5] S. McMurray, J. Kim, and C. C. Williams, "Quantitative measurement of two-dimensional dopant profile by cross-sectional scanning capacitance microscopy," J. Vac. Sci. Technol. B, 15, p. 1011, (1997).

[6] J. Kopanski, private communication.

[7] N. Duhayon, "Experimental study and optimization of scanning capacitance microscopy for two-dimensional carrier profiling of submicron semiconductor devices," Ph.D. thesis, (2006).

[8] V. Venezia, T. E. Haynes A. Agarwal, H. J. Gossmannc, and D. J. Eaglesham, "Enhanced diffusion of dopants in vacancy supersaturation produced by MeV implantation," Mater. Res. Soc. Symp. Proc., 469, p. 303, (1997).